Desalination and Water Treatment 322 (2025) 101134

Contents lists available at ScienceDirect

Desalination and Water Treatment

journal homepage: www.sciencedirect.com/journal/desalination-and-water-treatment/

Removal of amoxicillin, phenol, and diethyl phthalate using activated carbon from murici seeds (Byrsonima crassifolia L. Kunth)

Taynara Alvares Martins [a], Beatriz Carolina Alvez Tovar [b,*], Julião Pereira [a], Fernando Pereira de Sá [c], Tatianne Ferreira de Oliveira [a]

[a] School of Agronomy, Federal University of Goiás-UFG, Samambaia Campus, Goiânia, GO CEP 74690-900, Brazil
[b] Institute of Experimental Biology, Faculty of Sciences, Central University of Venezuela-UCV, Capital District Caracas, Venezuela
[c] Federal Institute of Education, Science and Technology of Goiás, Inhumas Campus, Inhumas, GO CEP 75402-556, Brazil

HIGHLIGHTS

- Adsorbent from murici seed removes 97 % diethylphthalate, 76 % amoxicillin and 56 % phenol.
- Chemically activated carbon from murici seeds yield a surface area of 556.97 m^2/g.
- Sustainable agro-waste use helps reduce environmental impact.
- Mesoporous murici adsorbent shows high efficiency in emerging contaminant removal.

GRAPHICAL ABSTRACT

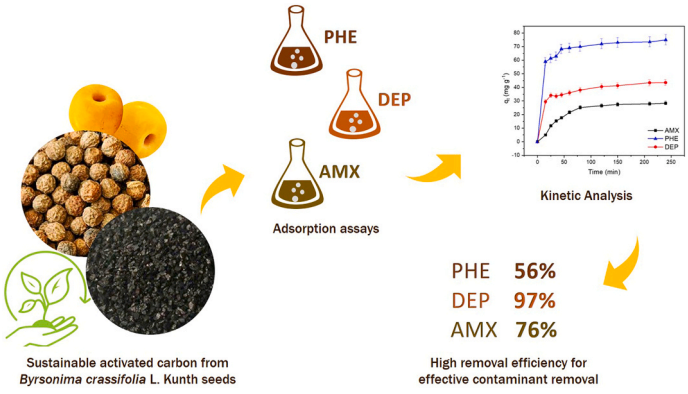

ARTICLE INFO

Keywords:
Byrsonima crassifolia: agricultural residues
Sustainable practices
Adsorbent material

ABSTRACT

The growth of anthropogenic activities, particularly the intensive use of pharmaceuticals and industrial chemicals, has led to the emergence of toxic "emerging pollutants," posing risks to ecosystems and public health. This study introduces a novel approach by converting murici seed, an underutilized agro-industrial waste, into an effective adsorbent for removing amoxicillin, phenol, and diethyl phthalate from water. Murici seeds were activated with phosphoric acid and carbonized. The activated carbon was characterized using electron microscopy, zero-point charge, infrared spectroscopy, thermal and textural analysis, revealing a surface area of 556.97 $m^2.g^{-1}$ pore volume of 0.447 $cm^3.g^{-1}$, and a mesoporous structure with an average pore diameter of 2.47 nm. A zero-point charge of 6.3 favors selective adsorption based on pH. The adsorbent achieved removal efficiencies of 76 % for amoxicillin, 56 % for phenol, and 97 % for diethyl phthalate, with maximum adsorption capacities (q_{max}) of 28.3 $mg.g^{-1}$ for amoxicillin, 74.9 $mg.g^{-1}$ for phenol, and 43.5 $mg.g^{-1}$ for diethyl phthalate. Most removal occurred within the first 60 minutes, attributed to the porous structure and oxygenated functional groups facilitating hydrogen bonding and π-π interactions. Compared to other agricultural waste-derived

* Corresponding author.
E-mail addresses: taynaramartinsa@gmail.com (T.A. Martins), beatrizcarolina.alveztovar@gmail.com (B.C. Alvez Tovar), racalele@ufg.br (J. Pereira), fernando.fpsa@ifg.edu.br (F.P. de Sá), tatianne_ferreira_oliveira@ufg.br (T.F. de Oliveira).

https://doi.org/10.1016/j.dwt.2025.101134
Received 2 September 2024; Received in revised form 13 February 2025; Accepted 17 March 2025
Available online 21 March 2025

adsorbents, murici-activated carbon shows superior efficiency, particularly for diethyl phthalate, highlighting its potential for scalable environmental remediation. This study offers a sustainable alternative for water purification and contributes to the circular economy by valorizing agro-industrial waste. The implications extend to cost-effective water treatment solutions in industrial and rural settings. Future research should explore adsorbent regeneration, reuse, and application in real-world wastewater systems to optimize performance and environmental benefits.

1. Introduction

The presence of emerging contaminants (CECs) in aquatic ecosystems has increased in recent years due to the release of pharmaceutical compounds and industrial chemicals. These contaminants, including pharmaceuticals, personal care products, biocides, illicit drugs, heavy metals, industrial and food additives pose significant risk to human health and biodiversity due to the persistence and bioaccumulative properties [1–4].

Health effects such as hormonal disruptions, antibiotic resistance, and cancer have been identified [5]. Substances like perfluoroalkyl and polyfluoroalkyl (PFAs) are associated with thyroid, kidney, and fetal development issues [6]. Microplastics, originating from various sources, impact marine life and animal health, entering the human food chain [7, 8]. Another type of contaminant is organic micropollutants found in pharmaceuticals, cosmetics, and biocides, which affect reproductive health and the nervous system [9].

In this study, three contaminants were selected for their distinct chemical properties and environmental persistence: amoxicillin (AMX), phenol (PHE), and diethyl phthalate (DEP). Amoxicillin, a widely used antibiotic, resists degradation, persisting in the environment and disrupting aquatic microbiota, thereby promoting antimicrobial resistance [10]. Phenol, an industrial chemical, is toxic at relatively low concentrations to both humans and aquatic organisms, impacting the nervous, respiratory, and hepatic systems due to its high solubility and persistence [11]. Diethyl phthalate, a common plasticizer, acts as an endocrine disruptor that bioaccumulates and mimics natural hormones, potentially causing infertility, developmental disruptions, and malformations in humans and wildlife [12]. The persistence and bioactivity of these contaminants pose challenges for water treatment systems, as their chemical properties complicate effective removal and increase the risk of continuous exposure.

Addressing the increasing issue of CECs involves a range of approaches, including membrane filtration [13], biological treatments [6], advanced oxidation processes [14], adsorption [15–19], and the use of wetlands [3]. Among these, adsorption is recognized as a particularly effective method for removing trace contaminants, providing opportunities for the recovery, reutilization, and reprocessing of adsorbent materials. Commercial activated carbons are effective against various CECs such as pesticides and pharmaceuticals in water streams [20], demonstrating efficiency in removing ciprofloxacin [9], or combinations of activated carbon with ultrasound irradiation and filtering membranes in removing diclofenac, carbamazepine, and amoxicillin [21]. However, the widespread use of commercial activated carbons faces several challenges, including high production costs, dependence on non-renewable resources, secondary pollution, limited regeneration efficiency, and variable performance across different contaminants [22]. These limitations highlight the need for alternative adsorbent materials derived from sustainable sources.

Recently, agricultural residues have increasingly been utilized in adsorption techniques to eliminate heavy metals, antibiotics, and other CECs [13,23]. The generation and management of these residues cause various environmental damages, including disease spread, unpleasant odors [24], insect and rodent proliferation [25], landscape degradation [26], and soil and water contamination [17,27]. Thus, it is crucial to develop innovative methods to convert these residues into carbon-based adsorbents, given their rich composition in lignin, cellulose, and hemicellulose [24–26]. For example, fruit peels such as orange [17,28], coconut [29], nuts [30,31], grape seeds [32], baru and monguba shells [27], as well as wood [33,34], have been explored for the removal of heavy metals an others contaminants [23,27,33]. Additionally, murici seeds have shown efficacy in removing heavy metals [23,35], organic dyes [36,37], metformin [15], antibiotics [16], among others [13,38].

Previous work by Martins et al. [39] explored the potential of murici and jabuticaba seed residues activated with phosphoric acid for adsorption of various CECs, focusing on surface characteristics and adsorption efficacy at different pH levels. These findings indicated the seeds promising potential for water treatment applications, with a specific emphasis on the role of surface acidity and porosity in contaminant removal. However, there remains a need to further explore how these surface characteristics interact with individual contaminants under varying conditions. This study thus seeks to advance this line of inquiry by concentrating on murici seeds, analyzing their physicochemical properties, adsorption capacity, and kinetic behavior, with particular emphasis on their rapid and efficient contaminant removal response.

The fruit of *Byrsonima crassifolia* L. Kunth [36], known as murici, yellow nanche, changunga, nance or peralejasu, is a fleshy, globular drupe measuring 1.5–2 cm in diameter [40]. Its color shifts from bright yellow to orange upon ripening, with a distinctive aroma resembling aged cheese. It features a dense, sweet-tart flesh surrounding a large, hard seed [40]. The fruit is rich in fiber, carbohydrates, unsaturated fatty acids, antioxidants, iron, and vitamin C, though low in protein [40, 41]. It is traditionally used in a wide range of products like sweets, jams, beverages, and ice cream. Despite its broad applications, the seeds are often discarded as waste, representing 25–34 % of the fruit's weight. These seeds hold great potential for valorization as agro-industrial by-products [42,43].

This study aims to convert murici seeds into sustainable adsorbent material, analyzing their physicochemical properties, adsorption capacity, and kinetic behavior in water treatment.

2. Experimental

2.1. Materials and samples

Phosphoric acid (purity > 85,0 %) was purchased from Neon (Suzano, SP, Brazil). The Amoxicillin (purity > 87,1 %) was acquired from Neo Química (Anápolis, GO, Brazil). The Phenol (Sol. 90 %) was purchased from Dinâmica (Indaiatuba, SP, Brazil). The Diethyl phthalate (purity > 99,0 %) was acquired from Sigma Aldrich (Barueri, SP, Brazil). Table 1 presents the chemical properties of the contaminants—amoxicillin, phenol, and diethyl phthalate—obtained from the PubChem database (National Center for Biotechnology Information) [44–46], which will serve as adsorbates in the study, as well as their structural properties modeled using ChemSketch (Freeware) 2023.2.4 [47].

The samples of murici (*Byrsonima crassifolia*) were donated by the company "Frutos do Brasil" (Abadia de Goiânia, GO, Brazil). These samples were processed to remove husk residues and impurities, leaving only the seeds. The seeds were then dried in an oven at 100°C for 24 hours. After drying, a mill was used to crush the seeds (Alfa Mare, AM 700), then sieved to separate the particles using 1.41 mm mesh screens (Granutest).

2.2. Activated carbon preparation process

For the production of activated carbon from murici seeds, the methodologies from [39,48,49] were combined. The process involved chemical activation with phosphoric acid (H_3PO_4), followed by carbonization. To begin, approximately 20 g of crushed seeds were immersed in 200 mL of 85 % H_3PO_4 and stirred continuously for 24 hours [50]. Then, 6 g of dry material were placed in a muffle furnace (JUNG, LF0610) and gradually heated at a rate of 30 ºC per minute up to 600 ºC, where it was maintained for 40 minutes, under a nitrogen gas flow of 2 L.min^{-1}. The carbonization process in a muffle furnace involved heating the material in a closed chamber, where oxygen access was completely eliminated. After heating, the material was cooled in a desiccator for 24 hours. Subsequently, the material was washed with a 0.1 mol.L^{-1} sodium hydroxide (NaOH) solution until the pH reached 6.5 to remove any residual activating agent. The final step involved drying the material at 110 ºC inside an oven for 24 hours. The percentage yield (Y) of the samples was estimated according to Eq. 1 [37], where xo is the weight of the precursor material (g) and x1 weight of the activated carbon (g).

$$Percentage\ yield\ Y(\%) = \frac{X1}{Xo} * 100 \quad (1)$$

2.3. Characterization of activated carbon

The surface and structural characterization of murici activated carbon follows the methods established in previous studies [39]. The thermal properties were evaluated using a thermogravimetric analyzer (SHIMADZU, DTG 60/60H). Thermogravimetric (TGA) and differential thermal analysis (DTA) curves were obtained in the temperature range between 25 and 1000 °C, with a 10 °C per minute heating rate, under nitrogen gas flow, and using alumina crucibles.

Subsequently, the morphological characteristics were examined employing a Scanning Electron Microscope (JEOL, JSM – 6610), fitted with EDS and Thermo Scientific NSS Spectral Imaging capabilities.

To analyze the point of zero charge (pH_{PZC}), the methodology proposed by Park and Regalbuto [51] was followed. Initially, 20 mL of NaCl solution (0.1 mol.L^{-1}) was prepared for each of the 11 different pH conditions (1−11). The pH of these solutions was adjusted using 0.1 mol.L^{-1} solutions of HCl or NaOH. Subsequently, 50 mg of the adsorbent material was added to each solution. The mixtures were then stirred for 24 hours at 25 °C and 125 rpm. The final pH of each solution was determined with the help of a laboratory pH analyzer (PHS-3E-B1, Atra).

The surface functional groups of the activated carbon were analyzed using Fourier-transform infrared spectroscopy (FT-IR) with a spectrophotometer (PERKINELMER, Spectrum 400). The range for the infrared analysis was set between 4000 and 400 cm^{-1}, with a resolution of 4 cm^{-1}. The samples were first dried at 110 °C for 24 hours. They were then blended with KBr and formed into pellets for the spectroscopic examination.

Finally, the textural properties were determined through nitrogen adsorption/desorption measurements (ASAP 2020, Micromeritics). The samples were pre-treated *in-situ* with a rate of temperature increase set to 10 °C per minute, under a N_2 flow at 30 °C for 10 minutes to eliminate surface contaminants and moisture. A 0.20 g of this pre-treated sample was then subjected to measurements at −196.15 °C to evaluate N_2 adsorption/desorption. The specific surface was determined from the Brunauer, Emmett, and Teller method, and the pore size distribution was

Table 1
Representation of the connectivity and molecular formulas of the pollutants studied.

PROPERTIES	Diethyl Phthalate (DEP)	Phenol (PHE)	Amoxicillin (AMX)
IUPAC name	diethyl benzene-1,2-dicarboxylate	benzenol	(2S,5R,6R)-6-[[(2R)-2-amino-2-(4-hydroxyphenyl)acetyl]amino]-3,3-dimethyl-7-oxo-4-thia-1-azabicyclo[3.2.0]heptane-2-carboxylic acid
Chemical Structure Model and dimensions by ACD/ChemSketch (Freeware) 2023.2.4	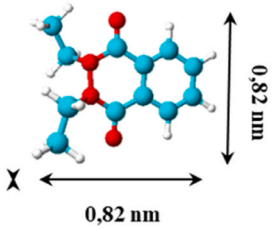	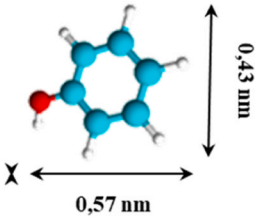	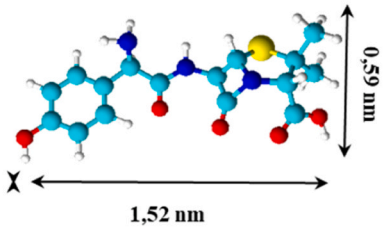
Molecular fórmula	$C_{12}H_{14}O_4$	C_6H_6O	$C_{16}H_{19}N_3O_5S$
Molecular weight	222.24 g/mol	94.11 g/mol	365.4 g/mol
Chemical safety			

Spheres represent the following elements: Carbon (C) in cyan, Hydrogen (H) in white, Oxygen (O) in red, Nitrogen (N) in blue and Sulfur (S) in yellow.

calculated using the Barrett, Joyner, and Halenda method [52].

2.4. Adsorption assays for Amoxicillin, Phenol, and Diethyl Phthalate

The adsorption experiments were conducted following a previously established methodology for evaluating adsorption capacity, adapted in this study to focus on kinetic analysis [39]. To analyze the concentration of amoxicillin (AMX), phenol (PHE), and diethyl phthalate (DEP), a UV-Vis spectrophotometer (SHIMADZU, UV-1800) was used. To determine the maximum absorption wavelengths for each contaminant, a spectral scan was conducted, resulting in $\lambda = 229$ nm for AMX, 265 nm for PHE, and 228 nm for DEP. Following this, various concentrations of AMX, PHE and DEP, were prepared by diluting aqueous solutions of the pollutants, which were then used to create calibration curves.

To evaluate the adsorption capacity of the activated carbon, adsorption experiments were conducted at 25 °C and pH 7 using 200 mL flasks. Each flask contained 50 mL of solutions of AMX, PHE, and DEP, with an initial concentration of 0.2 $g.L^{-1}$. To these solutions, 0.2 g of activated carbon from murici was added, following the methodology described in [14]. The experiments were carried out for 240 minutes (4 hours) in three replicates. The adsorption capacity (qe) and removal rate (R) were determined using Eqs. 2 and 3, respectively:

$$\text{Removal rate}\mathbf{R}\quad(\%) = \frac{(C_0 - C_f)}{C_0} \quad * \mathbf{100} \tag{2}$$

$$\text{Adsorption capacity}\boldsymbol{q_e}\quad (mg.g^{-1}) = \frac{\boldsymbol{V}(C_0 - C_f)}{\boldsymbol{m}} \tag{3}$$

The removal rate is expressed in percentage, while C_0 represents the initial concentration of the adsorbate, and C_f represents the final concentration in response to adsorption process (both concentrations in g. L^{-1}). In the case of adsorption capacity (q_e), represented in mg of adsorbate per g of adsorbent, V is the volume of the solution (L), and m is the mass of the adsorbent (g).

Kinetic analysis was performed using the pseudo-first order model represented by (Eq. 4); pseudo-second order (Eq. 5), and intraparticle diffusion of Webber-Morris (Eq. 6).

$$\text{Pseudo}-\text{first order}\frac{dq_t}{dt} = k_1(q_e - q_t) \tag{4}$$

$$\text{Pseudo}-\text{second order}\frac{dq_t}{dt} = k_2(q_e - q_t)^2 \tag{5}$$

$$\text{Webber}-\text{Morris}q_t = k_3 t^{\frac{1}{2}} + c \tag{6}$$

Where qe is the amount of solute adsorbed per unit mass of adsorbent (mg g^{-1}); qt is the amount of solute adsorbed per unit mass of adsorbent (mg g^{-1}) at time t (min); k1 is the pseudo-first order kinetic constant (min^{-1}); k2 is the pseudo-second order kinetic constant (g $mg.min^{-1}$); k3 is the intraparticle diffusion kinetic constant (mg g^{-1} $min^{-1/2}$), and c is the constant related to the thickness of the internal or external diffusion layer (mg g^{-1}).

3. Results and Discussion

3.1. Byrsonima crassifolia L. Kunth processing

A batch of ripe murici fruit (*Byrsonima crassifolia* L. Kunth), kindly provided by the pulp and ice cream processing company "Frutos do Brasil," underwent manual separation, resulting in pulp and seeds. The pulp was stored in polyethylene bags and frozen at −18 °C for future analysis of its components with potential nutraceutical applications. The seeds, after being dried, crushed, and subjected to a carbonization process, yielded 42 % (Fig. 1). Therefore, 8.4 g were recovered from the initial 20 g subjected to carbonization. This yield indicates a successful conversion of seed material into activated carbon, which may have significant applications in environmental remediation and adsorption processes due to its high surface area and porosity. During the activation processes, whether chemically or physically, lignocellulosic materials disintegrate through two stages: degradation of cellulose and hemicellulose, which leads to the formation of pores on the carbon surface and promotes the dispersal of the oxidizing agent, followed by the interaction of lignin with the oxidizing agent to produce AC. It can be concluded that the removal of volatile materials and the reaction that occurred between sample and activator are the main reasons for the reduction of AC yield [37].

3.2. Characterization of activated carbon

To assess how the behavior of adsorbent materials varies with temperature changes, thermogravimetric (TGA) and differential thermal analysis (DTA) were conducted on murici activated carbon. From the graphs in Fig. 2, it can be observed that the dynamic behavior concerning the increase in temperature was only reflected in the variation of mass loss.

Thermogravimetric analysis showed a mass loss exceeding 55 % for the murici activated carbon from 25 °C to 1000 °C. This analysis identified three decomposition phases similar to those reported by Sanchez et al. [43]. The first phase, from 25 °C to 150 °C, involves a 10 % mass

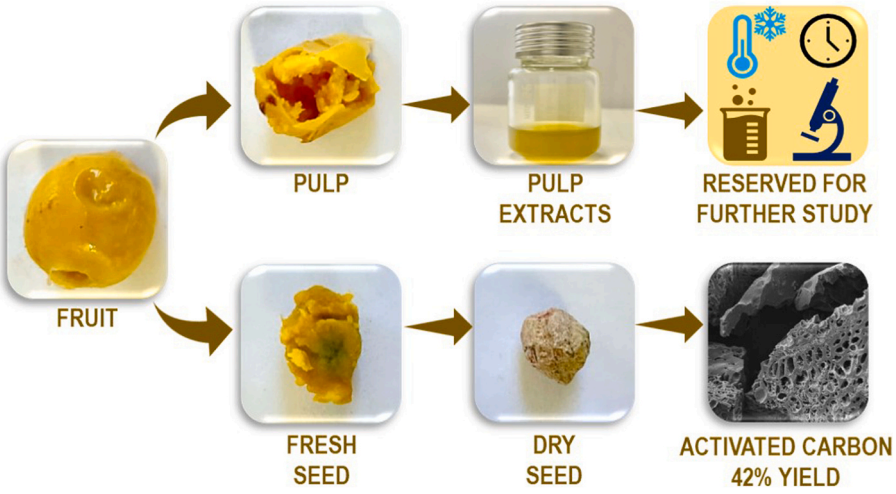

Fig. 1. Scheme of murici *(Byrsonima crassifolia* L. Kunth) sample processing and yield. The pulp was used to obtain plant extracts, while the fresh seeds were dried and subsequently activated to produce activated carbon.

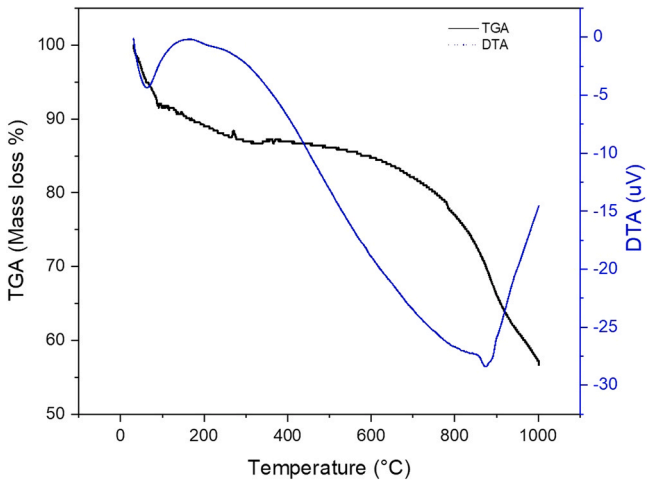

Fig. 2. Thermogravimetric analysis (TGA) and Differential Thermal Analysis (DTA) of activated carbon from murici. The TGA profile shows mass loss as a function of temperature, indicating the stages of thermal decomposition, while the DTA highlights the associated thermal transitions.

loss due to moisture and low molecular weight volatiles [53]. The second phase, from 150 °C to 450 °C, shows stability with hemicellulose decomposing between 180 and 270 °C and cellulose between 270 and 400 °C, releasing light organic compounds and gases [43,54,55]. The final phase, from 450 °C to 900 °C, results in about 30 % mass loss due to carbonate decomposition and significant structural changes [56,57].

Fig. 3 illustrates the structural profiles and morphology of activated carbon from murici. The SEM images reveal a highly porous surface with a honeycomb-like structure [32,39,58]. The scale bar of 50 μm highlights that the pores are smaller than this dimension, underscoring the material's micro-scale porosity. This interconnected pore network likely enhances the available surface area for adsorption, allowing for multi-directional diffusion pathways for adsorbates. The surface's rough texture and varying pore sizes may further contribute to an increased adsorption surface area by providing additional active sites. Despite the high porosity, the carbon structure remains intact and robust, indicating its suitability for adsorption applications.

An important parameter for characterizing the surface of activated carbons is the point of zero charge (PZC), through which it is possible to determine, as a function of pH, the tendency of a surface to become positively or negatively charged, favoring the adsorption of anions or cations. The type and quantity of functional groups present on the adsorbent cause this value to vary [34]. Fig. 4 shows pH_{PZC} graphs for murici activated carbon, which is 6.3. At pH levels below this, the carbon surface carries a positive charge and attracts anions, whereas at higher pH levels, it becomes negatively charged and consequently attracts cations [59]. This means that the carbon could adsorb anions when the pH is low and cations when the pH is high, although its ion exchange capacity may be low compared to other materials specifically designed for this purpose.

These findings align with the FT-IR results, indicating that the synthesized activated carbon predominantly possesses acidic properties. Fig. 5 presents the FT-IR spectra for murici activated carbon. By referencing existing studies and transmittance tables, the key vibrations corresponding to various functional groups in the material were identified. The FT-IR spectrum displays bands between 2800 and 3000 cm^{-1}, associated with C-H stretching in methyl (-CH_3) and methylene (-CH_2-) groups, indicating aliphatic groups on the activated carbon surface [15,34]. The band near 1743 cm^{-1} corresponds to C═O stretching, suggesting the presence of carbonyl groups such as carboxylic acids, ketones, and esters [15]. Bands in the 1500–1600 cm^{-1} range are linked to C═C stretching in aromatic rings and N-H bending in amines, indicating aromatic structures and possible amines on the surface [16,58]. Vibrations between 950 and 1200 cm^{-1} are attributed to C-O stretching in hydroxyl groups of alcohols, esters, and ethers [15,60]. Finally, bands between 900 and 700 cm^{-1} are typically linked to out-of-plane C-H bending in aromatic rings, further confirming the presence of aromatic structures in murici activated carbon [16,34]. These groups tend to make the carbon more hydrophilic, as they allow for the formation of hydrogen bonds with water molecules. The presence of aliphatic and aromatic groups can impart certain hydrophobic characteristics, but the high proportion of oxygen suggests that murici carbon is relatively hydrophilic.

The FT-IR analysis provides valuable insight into the interactions between amoxicillin, phenol, and diethyl phthalate molecules and the surface of murici-based activated carbon by revealing the chemical functions present in each molecule and their relationship with the functional groups identified on the carbon. Amoxicillin, an antibiotic, contains functional groups such as amines, which can form hydrogen bonds with carboxylic groups (C═O) on the carbon surface.

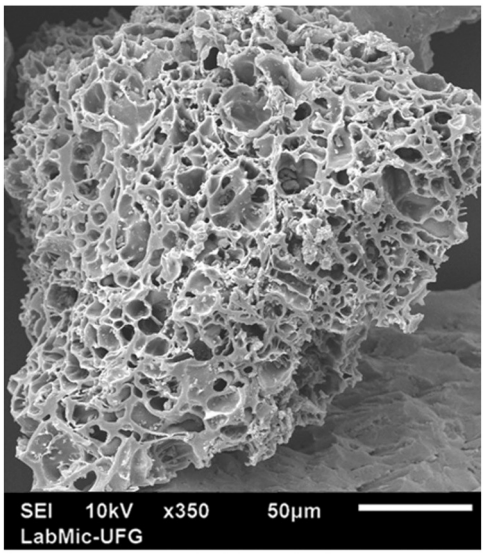

Fig. 3. Scanning Electron Microscopy (SEM) image of the porous structure of murici activated carbon before the adsorption process. The analysis conditions were 10 kV and 350x magnification.

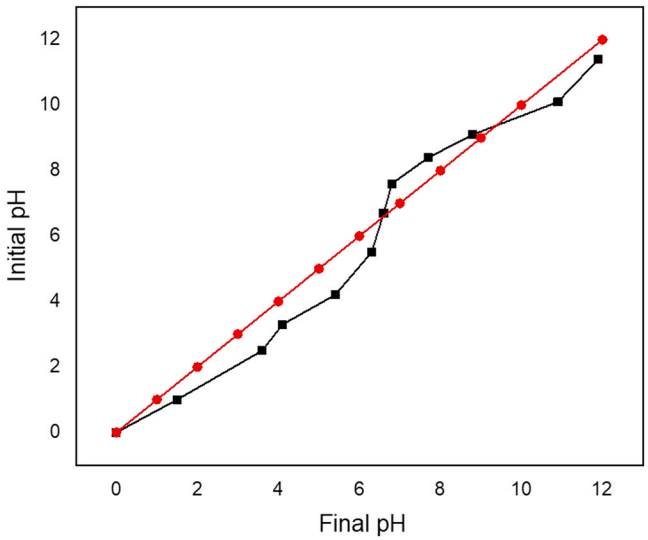

Fig. 4. Determination of the point of zero charge (pH_{PZC}) of murici activated carbon using the pH drift method. The intersection curve indicates the pH at which the materials surface has no net charge.

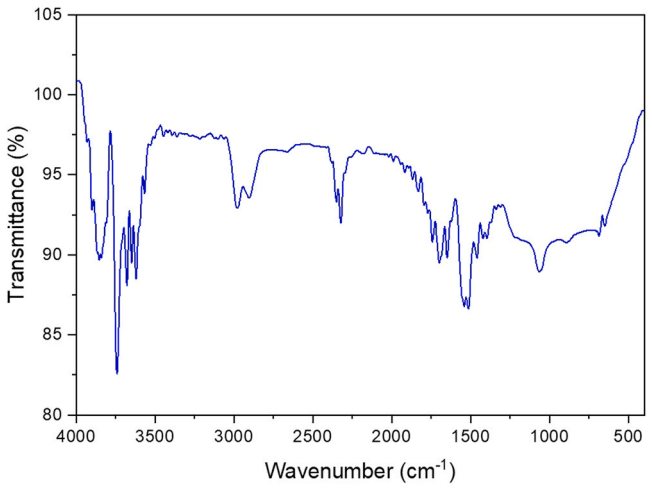

Fig. 5. Fourier-transform (FT-IR) spectral curve of infrared absorption by transmittance for activated carbon from murici, identifying the functional groups present on the material's surface.

Additionally, it features a β-lactam group and an aromatic system, typical of penicillin-family antibiotics, which may interact with the aromatic structure in murici-based activated carbon, facilitating adsorption through van der Waals (π-π) interactions [10,18,61]. Phenol, with its hydroxyl group (-OH), imparts acidic and polar characteristics, enabling hydrogen bond formation with the activated carbon surface, thus enhancing adsorption [11,26,31]. Diethyl phthalate, an ester, contains carbonyl groups that can interact with the carbonyl groups on the activated carbon through hydrogen bonding, while its aromatic system can engage in π-π interactions with the aromatic structures of the carbon, facilitating retention [12,62–64]. The diverse functional groups on the activated carbon surface provide a range of binding capabilities, increasing its effectiveness in adsorbing organic compounds and highlighting murici-based activated carbon as a low-cost material with promising potential for water purification and wastewater treatment applications.

The interaction between the pollutants and the functional groups on the surface of murici activated carbon is influenced by the chemical properties and the polar or nonpolar nature of the molecules. In the case of amoxicillin (AMX), this molecule contains several functional groups with different charges at different pH levels, which affects its behavior towards the groups on the surface of the carbon. At pH 7, amoxicillin adopts a zwitterionic form, which allows its amino group ($-NH_3^+$) to form dipolar interactions with the phenolic (-OH) groups of activated carbon [16,65], while its carboxylate group ($-COO^-$) may experience repulsion from the carbonyl groups (C═O) on the surface of the carbon, reducing amoxicillin's affinity for the adsorbent material compared to other pollutants. Regarding phenol (PHE), due to its aromatic structure and the presence of a hydroxyl group (-OH), hydrogen bonding between the phenol -OH group and the carbonyl (C═O) groups of activated carbon is favored [31]. Additionally, the aromatic structure of both phenol and activated carbon can induce π-π interactions between the benzene rings, facilitating phenol adsorption on the material's surface [26]. On the other hand, diethyl phthalate (DEP), a non-ionizable molecule with a more complex steric structure, exhibits a more pronounced interaction with the carboxyl (-COOH) and carbonyl (C═O) groups of activated carbon through hydrogen bonding between the DEP -OH group and these functional groups [63,64]. Non-covalent interactions, such as hydrogen bonds and π-π interactions, significantly contribute to the high adsorption capacity of these pollutants, especially in conditions where the carbon surface is moderately negatively charged, favoring the adsorption of neutral or slightly positively charged compounds [16,31,66–68]. These interaction mechanisms highlight the versatility of murici activated carbon in adsorbing a variety of organic pollutants, from ionizable compounds like amoxicillin to non-ionizable molecules like phenol and phthalate, making this material an efficient and eco-friendly option for pollutant removal in aquatic systems.

The BET method revealed a specific surface area of 566.970 $m^2.g^{-1}$, while the total pore volume measured by the BJH method was 0.351 $cm^3.g^{-1}$, with micropores accounting for 0.033 $cm^3.g^{-1}$ and mesopores for 0.318 $cm^3.g^{-1}$, as detailed in Table 2. The analysis of textural properties showed that the average pore diameter for murici activated carbon was 2.47 nm, which is adequate for adsorbing molecules of AMX, PHE, and DEP with diameters of 0.82, 1.52, and 0.57 nm, respectively. This porous distribution is crucial for the adsorption of contaminants of varying sizes. In the case of murici-derived activated carbon, the higher proportion of mesopores enhances the diffusion and accessibility of larger molecules, such as phenol (PHE, 1.52 nm) and amoxicillin (AMX, 0.82 nm), to internal active sites, resulting in increased adsorption capacity. Conversely, micropores play a significant role in the adsorption of smaller molecules, such as diethyl phthalate (DEP, 0.57 nm), by providing a highly active internal surface. Moreover, the synthesized carbon displayed a greater proportion of mesopores compared to micropores, enhancing the movement of molecules to internal adsorption sites. The balanced combination of mesopores and micropores in our material not only broadens the range of contaminants that can be efficiently adsorbed but also optimizes the adsorption kinetics by reducing diffusion resistance. These results underscore the material's excellent adsorptive capabilities.

Physisorption with inert gas (N_2) is one of the most common and effective ways to determine the specific surface area of porous materials. Fig. 6 displays the isotherms for nitrogen adsorption and desorption of murici activated carbon sample. The occupation of larger pores and the external surface is evidenced by the substantial increase in the adsorbed volume as the relative pressure increases [69]. Such a pattern suggests that the material mainly exhibits a mesoporous structure, aligning with the BJH method's pore size distribution results. In applications involving the liquid phase, such as the adsorption of several macromolecules, the presence of mesoporosity is often more advantageous than microporosity [16,70].

The activation of carbon with acidic substances creates a rigid, porous matrix with cross-linking and oxidizes the surface, thereby increasing its acidity and the number of negatively charged functional groups. This enhances the electrostatic attraction between the sorbent and various sorbates. High-temperature pyrolysis following acid activation forms meso- and macropores, improves surface oxidation, and reduces the risk of pore collapse, thus optimizing porosity [66], features observed in murici carbon activated with H_3PO_4.

To contextualize the performance of murici-activated carbon, a comparison with other activated carbons derived from agricultural wastes is presented in Table 3. The transformation of agricultural waste materials into activated carbons highlights the influence of both the raw material and the activating agent on the final textural properties. For instance, murici seeds activated with H_3PO_4 yielded a surface area of 556.97 $m^2.g^{-1}$ and a pore size of 2.47 nm, which is comparable to lemon peel activated with CO_2 (1018.52 $m^2.g^{-1}$, 2.78 nm) [17] and macadamia nutshells activated with K_2CO_3 (1225.00 $m^2.g^{-1}$, 0.406 nm) [58]. These results suggest that the choice of activating agent plays a critical role in determining the pore structure and surface area. Acidic agents like H_3PO_4 tend to produce carbons with a balanced distribution of mesopores and micropores, as seen in murici and *Miscanthus* × *giganteus* [71] (1368.00 $m^2.g^{-1}$, 4.01 nm), while alkaline agents like KOH and K_2CO_3 can lead to highly microporous structures, as observed in macadamia nutshells (0.406 nm) [58] and Brazil nutshells (3.69 nm) [31].

The pore size distribution is particularly important for adsorption applications. Murici-activated carbon, with its average pore size of 2.47 nm, is well-suited for adsorbing molecules like AMX, PHE, and DEP, which have diameters below 2 nm. In contrast, materials with larger pore sizes, such as grape marc (10.29 nm) [32], may be more suitable for adsorbing larger molecules or macromolecules. However,

Table 2
Textural properties in activated carbon from murici.

Measures	AS_{BET} ($m^2.g^{-1}$)	V_{Tpores} ($cm^3.g^{-1}$)	$V_{Mesopores}$ ($cm^3.g^{-1}$)	$V_{Micropores}$ ($cm^3.g^{-1}$)	Mesopores (%)	Micropores (%)	Average $_{pore\ diameter}$ (nm)
Murici	566,970	0351	0318	0033	90,59	9,41	2476

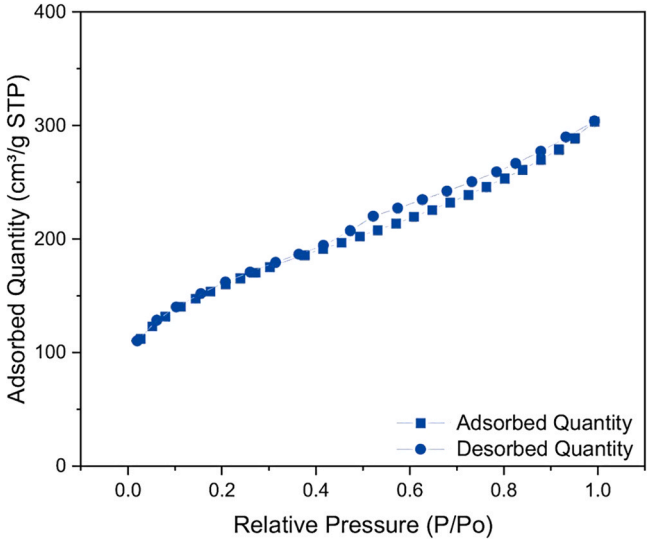

Fig. 6. Nitrogen adsorption/desorption isotherm at −196.15 °C for murici activated carbon obtained through specific surface area analysis (ASAP). The curve indicates a mesoporous structure, and the surface area was calculated using the BET model.

the lower surface area and pore volume of grape marc (44.23 $m^2.g^{-1}$, 0.305 $cm^3.g^{-1}$) [32] limit its overall adsorption capacity compared to murici-activated carbon.

The influence of the activating agent is further evidenced by the results of Sanchez et al. [15], who used NaOH to activate murici seeds and obtained a much lower surface area (43.30 $m^2.g^{-1}$) compared to our work (556.97 $m^2.g^{-1}$). This stark difference underscores the importance of selecting an appropriate activating agent to optimize the textural properties of the carbon. Similarly, the use of CO_2 as an activating agent for lemon peel resulted in a high surface area (1018.52 $m^2.g^{-1}$) [17] and a pore size of 2.78 nm, demonstrating the versatility of CO_2 in creating mesoporous structures.

While materials like *Miscanthus* × *giganteus* [71] and waste wood [33] showcase exceptional textural properties (1368.00 $m^2.g^{-1}$ and 2230.00 $m^2.g^{-1}$, respectively), their practical application may be limited by factors such as raw material availability, processing complexity, and environmental impact. In contrast, murici seeds offer a sustainable and low-cost alternative, particularly in regions where this agricultural waste is abundant. Although macadamia nutshells (1225.00 $m^2.g^{-1}$, 0.801 $cm^3.g^{-1}$) [58] also present strong adsorption potential, their use may be constrained by regional availability and higher costs. On the other hand, materials like grape marc [32] and Brazil nutshells [31] exhibit limited adsorption capacity due to their low surface area and pore volume, though they could still find niche applications. For example, Brazil nutshells activated with KOH (332.23 $m^2.g^{-1}$, 0.020 $cm^3.g^{-1}$) [31] show potential for applications requiring microporous materials, despite their lower surface area.

Overall, murici-activated carbon emerges as a promising material, striking a balance between performance, cost-effectiveness, and sustainability. Its moderate surface area, combined with a mesoporous structure and a pore size suitable for adsorbing a wide range of pollutants, positions it as a versatile adsorbent for environmental remediation. Furthermore, the use of H_3PO_4 as an activating agent not only enhances the material's textural properties but also introduces oxygenated functional groups that improve its affinity for polar pollutants. To further enhance its competitiveness, future studies should focus on optimizing the activation processes to improve its textural properties while maintaining its low-cost and sustainable advantages.

In summary, murici-based activated carbon presents favorable characteristics for environmental remediation applications, particularly in the adsorption of emerging contaminants. Its moderately hydrophilic nature, as indicated by FT-IR results showing oxygenated functional groups (e.g., carbonyl and hydroxyl groups), enhances its ability to form hydrogen bonds, allowing efficient interaction with water and dissolved pollutants. While the presence of aliphatic and aromatic groups introduces some hydrophobic characteristics, the high proportion of oxygen-rich groups suggests an overall hydrophilic tendency, beneficial for aqueous-phase applications. Additionally, its pH-dependent charge properties, with a point of zero charge (pH_{PZC}) of 6.3, allow for selective ion adsorption. Below this pH, the carbon surface becomes positively charged, promoting anion attraction, while at higher pH levels, the surface becomes negatively charged, favoring cation adsorption. Although its ion exchange capacity may be more limited than that of highly functionalized materials, murici activated carbon still demonstrates versatile adsorption capabilities due to its surface chemistry and pore structure, positioning it as a cost-effective and promising option for water purification and pollutant removal.

3.3. Assessment of adsorption and kinetic model fitting

In this study, the activated carbon exhibited notable efficiency in removing emerging contaminants, achieving high removal rates: 76 % for AMX, 56 % for PHE, and an impressive 97 % for DEP. These results underscore the material's effectiveness in pollutant adsorption, with maximum adsorption capacities reaching 28.3 $mg{\cdot}g^{-1}$ for AMX, 74.9 $mg{\cdot}g^{-1}$ for PHE, and 43.5 $mg{\cdot}g^{-1}$ for DEP (Fig. 7).

This study focuses on the use of murici seeds (*Byrsonima crassifolia* L. Kunth), an underutilized agricultural waste, for the production of

Table 3
Comparison of textural properties of activated carbons derived from agricultural wastes.

Activated carbon	AS_{BET} ($m^2.g^{-1}$)	V_{Tpores} ($cm^3.g^{-1}$)	Pore size (nm)	Activating agent	Reference
Murici seeds	556.97	0.351	2.47	H_3PO_4	This work
Miscanthus × *giganteus*	1368.00	0.920	4.01	H_3PO_4	Osman et al. [71]
Waste wood	2230.00	1.270	0.35	H_3PO_4	Strong et al. [33]
Macadamia nutshells	1225.00	0.801	0.406	K_2CO_3	Duque-Brito et al. [58]
Grape marc	44.23	0.305	10,29	N/A	Sağlam et al. [32]
Brazil nutshells	332.23	0.020	3.69	KOH	Da Silva et al. [31]
Murici seeds	43.30	N/I	N/I	NaOH	Sanchez et al. [15]
Lemon peel	1018.52	0.5377	2.78	CO_2	Mohamad et al. [17]

N/I = Not Informed; N/A = Not Applicable

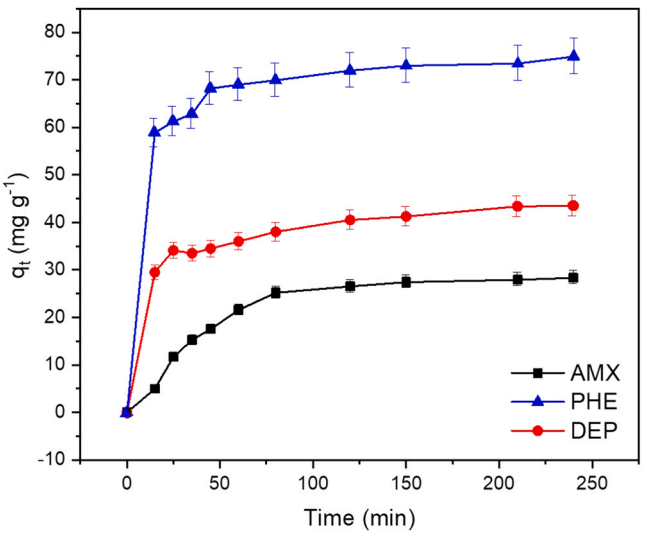

Fig. 7. Adsorption kinetic assays of AMX, DEP, and PHE on murici activated carbon. The graph shows the adsorbed amount (qt) as a function of time, highlighting differences in the adsorption capacity among the three contaminants.

activated carbon. While other studies have explored fruit seeds such as mango, avocado, or jabuticaba, murici offers a unique chemical composition and specific textural properties that favor the adsorption of three environmentally relevant pollutants: an antibiotic (amoxicillin), a phenolic compound, and a plasticizer (diethyl phthalate). Table 4 provides a comparative analysis of the adsorption performance of murici-activated carbon against other agricultural waste-derived adsorbents, considering not only the removal efficiency (%) but also the initial concentration of pollutants and the adsorption capacity (q_{max}, mg.g^{-1}).

The adsorption efficiency of murici-activated carbon for amoxicillin was 76 %, which is notably higher than that of vegetal powdered carbon (40 %) [61], *Prosopis juliflora* wood (46 %) [66], and jujube nuts (37 %) [30]. However, when considering adsorption capacity, *Prosopis juliflora* wood exhibits a significantly higher q_{max} (714.3 mg/g) at an initial concentration of 500 mg/L, while the q_{max} for murici-activated carbon is 28.3 mg.g^{-1} at 200 mg.L^{-1}. These differences highlight the strong influence of initial pollutant concentration on qmax values. Since adsorption efficiency tends to decrease at higher initial concentrations due to saturation of active sites, the performance of murici-activated carbon remains competitive, particularly when considering real-world applications where initial pollutant concentrations may vary widely.

For phenol adsorption, murici-activated carbon achieved an efficiency of 56 %, lower than that of rice husk (94 %) [11], and oak wood (99 %) [34],] and oak wood (99 %) [42], but comparable to sugarcane bagasse (66 %) [37]. Notably, the q_{max} of murici-activated carbon (74.9 mg.g^{-1} at 200 mg.L^{-1}) surpasses that of rice husk (20.9 mg.g^{-1} at 300 mg.L^{-1}), suggesting that, while efficiency values are lower, murici carbon maintains a competitive adsorption capacity. The lower efficiency may be attributed to differences in activation conditions and surface chemistry, reinforcing the need for optimization strategies to enhance performance for phenolic compound removal.

Regarding diethyl phthalate, murici-activated carbon exhibited outstanding performance, with a 97 % removal efficiency and a q_{max} of 43.5 mg.g^{-1} at 200 mg.L^{-1}. This is higher than the efficiency of cotton straw (78 %) [62] and comparable to that of the coal-chitosan composite (91 %) [67] and jabuticaba seeds (90 %) [39]. However, cotton straw demonstrated a remarkably high q_{max} (657.0 mg.g^{-1} at 50 mg.L^{-1}), emphasizing that adsorption capacity can be significantly affected by initial concentration and material properties.

These findings highlight the importance of considering both efficiency and adsorption capacity when comparing different adsorbents. While murici-activated carbon may not always achieve the highest q_{max} values, its ability to maintain high removal efficiencies even at relatively high initial concentrations supports its potential for practical applications. Furthermore, the unique textural and chemical properties of murici-derived carbon contribute to its versatility in adsorbing different classes of pollutants. This study not only demonstrates the feasibility of using murici seeds for activated carbon production but also underscores the need for standardized conditions when comparing adsorption performance across different materials.

The adsorption capacity of carbon is influenced by several parameters such as the structure, the texture, the nature of the surface, and the diameter of particles, particularly in the case of activated carbon obtained through chemical activation [34].

Recent studies have shown similar trends. For example, the research conducted by Laksaci et al. [16] exhibited remarkable adsorption efficiency, reaching 370 mg.g^{-1} for AMX removal via adsorption on activated carbon derived from coffee waste activated with KOH. Additionally, the study by Chandrasekaran et al. [66] focused on the use of *Prosopis juliflo ra* wood-derived carbon activated with H_3PO_4, similar to this work, for the adsorption of AMX. The activated carbon demonstrated a remarkable adsorption capacity of 714.29 mg.g^{-1}, suggesting that this behavior could possibly be influenced by the activating agent.

In their studies on AMX adsorption, El Azzouzi et al. [72] observed a maximum adsorption capacity of 26 mg.g^{-1} in less than 60 minutes, using another type of adsorbent material, a kaolinite. Belaissa et al. [30] found optimal AMX removal using activated carbon derived from jujube nuts, activated with H_2SO_4, achieving a maximum adsorption capacity of 70 mg.g^{-1} in approximately 70 minutes.

These results indicate that the use of different activating agents is directly related to the porous structure and, consequently, the adsorption capacity of activated carbon.

Regarding the removal of PHE, it is observed that the activated carbon from murici was more efficient when compared to the adsorption results of AMX and DEP. In the chemical activation process, H_3PO_4

Table 4
Comparison of adsorption efficiency of activated carbon from agricultural waste.

Pollutant	Initial concentration (mg.L^{-1})	Activated carbon	q_{max} (mg.g^{-1})	Efficiency (%)	Reference
Amoxicillin	200	Murici seeds	28.3	76	This work
	50	Vegetal powdered	87.0	40	Berges et al. [61]
	500	*Prosopis juliflora* wood	714.3	46	Chandrasekaran et al. [66]
	200	Jujube nuts	79.0	37	Belaissa et al. [30]
Phenol	200	Murici seeds	74.9	56	This work
	300	Rice husk	20.9	94	Kennedy et al. [11]
	100	Sugarcane bagasse	158.9	66	El-Bery et al. [37]
	100	Oak wood	250.0	99	Dehmani et al. [34]
Diethyl phthalate	200	Murici seeds	43.5	97	This work
	50	Cotton straw	657.0	78	Cheng et al. [62]
	10	Chitosan composite	42.7	91	Shaida et al. [67]
	200	Jabuticaba seeds	29.8	90	Martins et al. [39]

stands out as an activating agent, demonstrating greater efficiency in enhancing the adsorption properties of carbon compared to other acidic and basic agents. Unlike strong bases, which tend to reduce the adsorption capacity of treated carbon, H_3PO_4 not only facilitates an optimal porous structure but also significantly increases contaminant removal efficiency, such as phenol, achieving nearly 100 % elimination. This effectiveness makes H_3PO_4 preferable in water treatment applications, as it produces carbons with superior adsorption capacities, even surpassing those of commercial activated carbons [34].

The examination of the activated carbon's zero point of charge value of 6.3 reveals a greater presence of acidic functional groups on the surface, such as carbonyl, phenolic, carboxylic, and lactonic groups, indicating a predominantly acidic nature in activated carbons. Consequently, this results in a surface with a negative inclination since the pH_{PZC} (CA surface) is greater than the pH (aqueous phase), i.e., $6.3 > 7$. Therefore, the CA surface is negatively charged, favoring the attraction of anions [39].

Khraisheh et al. [68] investigated the adsorption of PHE with an initial concentration of 500 ppm. Their results indicated that the highest adsorption efficiency was 160.6 $mg.g^{-1}$, with a final concentration reduced to zero in approximately 10 minutes. Similarly, El-Bery et al. [37] utilized precursor materials such as sugarcane bagasse and sawdust, and by comparing two activating agents, K_2CO_3 and KOH, they determined that 158.9 $mg.g^{-1}$was the high adsorption capacity for phenol. In this regard, Xie et al. [73] found that the peak adsorption capacity occurred at an optimal pH of 7, in approximately 60 minutes, with a value of 169.9 $mg.g^{-1}$ when examining the process of phenol adsorption by commercial activated carbon. Dehmani et al. [34], analyzed the adsorption removal of PHE by activated carbon derived from oak wood charcoal and observed a qmax of 250 $mg.g^{-1}$ in less than 30 minutes. The carbon was activated using H_3PO_4, which is advantageous as this activating agent significantly enhances the porous surface, improving adsorption capacity. The ability to achieve effective adsorption in a short time is crucial for efficient water treatment applications

As illustrated in Fig. 7, the activated carbon demonstrated effective promotion of DEP removal, achieving optimal performance under these conditions, superior to that of AMX and lower than that of PHE. The researchers Shi et al. [64] analyzed the adsorption of DEP on biochars derived from six widely produced biomass wastes in China and reported a high adsorption capacity for coal-based activated carbon, with a qmax of 261 $mg.g^{-1}$. Similarly, Shaida et al. [67] investigated the removal of DEP through adsorption onto mineral-enriched residual coal modified with chitosan, finding that the adsorption efficiency reached 42.67 $mg.g^{-1}$.

Building upon the preliminary study by Martins et al. [39], this research emphasizes the importance of the activating agent used in the preparation of murici activated carbon and its significant impact on adsorption capacity and contaminant removal times for AMX, PHE, and DEP across various pH levels. These findings underscore the potential of this carbon for effective environmental remediation and highlight the need for further exploration in this area.

While this and other studies have focused on the adsorption of individual contaminants such as AMX, PHE, and DEP, it is important to acknowledge that in real-world scenarios, pollutants rarely occur in isolation. Instead, they are typically present as complex mixtures of various substances, which can significantly influence adsorption behavior. For example, Elsayed et al. [74] investigated the adsorption of heavy metals (Cu^{2+}, Ni^{2+}, and Co^{2+}) using hydrogel as an adsorbent, both individually and in a mixed system. Their findings revealed a slight decrease in adsorption capacity when metals were present in a mixture, highlighting competitive interactions between contaminants. They also emphasized that pH was the most influential factor in the adsorption process.

These insights suggest that competitive adsorption dynamics play a critical role in multi-contaminant systems. Therefore, we recommend that future studies explore the adsorption performance of murici-based activated carbon in multi-component systems to better simulate real environmental conditions and optimize treatment processes.

The evaluation of the kinetic models was conducted through the analysis of the determination coefficients (R^2) and the comparison between the experimental data and those predicted by the models (Table 5). The pseudo-second-order model showed the best fit for most tests, these results are similar to previous works for AMX [61], PHE [26, 37,73] and DEP [63,64,67]. According to Hu et al. [35], this model suggests that chemisorption may be the predominant reaction mechanism between the adsorbent and the adsorbate, involving electron exchanges or valence forces. The results of these authors, who analyzed phosphate adsorption onto activated carbon, also fit better with the pseudo-second-order model. Thus, the results obtained from the kinetic modeling indicate that chemisorption may occur due to the presence of acidic functional groups, such as carboxylic, phenolic, carbonyl, and ester groups on the surface of the synthesized carbons.

The results obtained show that murici activated carbon has a high affinity for phenol (PHE) and diethyl phthalate (DEP) compared to amoxicillin (AMX) at pH 7. This is explained in terms of the zero-charge point (pH_{PZC}) of the carbon (6.3) and the pKa values of the contaminants. At pH 7, the activated carbon has a slight negative charge on its surface, which favors the adsorption of neutral or positively charged compounds while potentially repelling anions. Since phenol is predominantly neutral (pKa ~9.95) [31], and DEP is non-ionizable, both exhibit a high adsorption capacity under these conditions, reaching q_{max} values of 74.9 $mg.g^{-1}$ for PHE and 43.5 $mg.g^{-1}$ for DEP, which are significantly high.

In contrast, AMX, with pKa values of 2.4, 7.4, and 9.6, tends to exhibit complex speciation at this pH, adopting a zwitterionic form ($–COO^-$ and $–NH_3^+$) [16,65]. This state may reduce its affinity for the carbon surface due to possible repulsion between the deprotonated carboxylate group of AMX and the negatively charged carbon surface, explaining the lower q_{max} value of 28.3 $mg.g^{-1}$ for AMX compared to PHE and DEP.

Finally, murici activated carbon, according to its physicochemical characterization, presents a moderately hydrophilic surface with oxygenated functional groups, such as carbonyls and hydroxyls, that allow for the formation of hydrogen bonds. Although the ion exchange capacity is relatively limited, these characteristics suggest that murici activated carbon is a versatile and effective adsorbent for non-ionizable and neutral compounds, making it a valuable material for applications in the removal of contaminants from aquatic systems. Additionally, its natural composition and its ability to efficiently adsorb contaminants highlight its potential as a sustainable and eco-friendly alternative in wastewater treatment.

3.4. *Economic feasibility and environmental considerations of H_3PO_4 activation*

Murici seeds, used as a precursor material for the production of activated carbon, do not represent an additional cost, as they are a waste donated by a local company. This approach not only reduces costs but also promotes the valorization of agro-industrial waste and encourages sustainable practices. In this study, laboratory-scale production had an

Table 5
R^2 values for kinetic models of AMX, PHE and DEP adsorption of activated carbon from murici.

Pollutant	Pseudo-first order (R_1^2)	Pseudo-second order (R_2^2)	Webber Morris (R_3^2)
Amoxicillin	0966	0981	0809
Phenol	0900	0979	0821
Diethyl phthalate	0846	0985	0795
Standard Deviation	0.0601	0.0031	0.0130

estimated cost of 1107.56 USD/kg, with a weekly production of 90 g. The cost is broken down into 36.74 USD for 85 % H_3PO_4, 5.40 USD for energy (local energy rate), 0.04 USD for water (local water rate), 50.00 USD for labor (local labor rate), and 7.50 USD for maintenance, totaling 99.68 USD per week. The high cost is primarily due to H_3PO_4 (37 %) and labor (50 %).

In the work of Strong et al. (2023), it was demonstrated that H_3PO_4 can be recycled, reducing costs and environmental impact. When using 25 % H_3PO_4, 87.5 ± 0.6 % of the acid was recovered, compared to 63.9 ± 1.6 % with 85 % H_3PO_4. This is because the more concentrated and viscous acid does not efficiently penetrate the precursor material, reducing its effectiveness. Based on these findings, production costs could be adjusted. By using 25 % H_3PO_4 and maximizing the use of the furnace (10 carbonizations per week), 500 g of seeds could be processed, yielding 225 g of activated carbon. Although water (0.1 USD, local water rate) and energy (13.50 USD, local energy rate) consumption increases, the cost would be reduced to 344.89 USD/kg at the laboratory scale. This reduction represents a significant advantage for industrial scaling, where higher processing volumes would further decrease costs.

The scalability of murici seed-derived activated carbon production presents both technical and economic challenges that must be addressed to facilitate industrial implementation. Technically, ensuring uniform carbon activation on a large scale requires precise control over parameters such as temperature, residence time, and acid concentration. The recovery and recycling of H_3PO_4, as suggested by Strong et al. (2023), become critical to both cost reduction and environmental sustainability. Additionally, energy efficiency is a key factor; transitioning from batch processes to continuous-flow reactors could enhance throughput while reducing energy costs. This cost reduction not only improves economic feasibility but also minimizes resource consumption, contributing to a more sustainable production process.

Economically, scaling up could benefit from economies of scale, particularly in raw material processing, energy consumption, and labor optimization. Integrating the production process with existing agro-industrial operations that generate murici seed waste can further reduce logistical costs and promote a circular economy model.

For industrial-scale implementation, we propose the following strategies: 1) Implementing closed-loop acid recovery systems to maximize H_3PO_4 reuse, thus significantly lowering operational costs and minimizing environmental impact. 2) Utilizing continuous-flow reactors for carbonization and activation processes to improve energy efficiency and production consistency. 3) Partnering with local agro-industrial companies to secure a steady supply of murici seeds, reducing raw material costs and promoting waste valorization. 4) Incorporating waste heat recovery systems to utilize excess heat generated during the activation process, further improving overall process efficiency. These strategies not only address the scalability challenges but also align with sustainable production practices, enhancing the feasibility of murici seed-derived activated carbon in industrial applications.

In addition to the economic and technical scalability, the environmental sustainability of the activation process is equally critical. Evaluating the life cycle impacts of the materials and methods used provides a comprehensive understanding of their long-term feasibility and environmental footprint. Choudhry et al. [75], in their work on the chemical activation of cotton fibers, evaluated the effect of four reagents (H_3PO_4, $ZnCl_2$, KOH, and $K_2C_2O_4$) on the morphology of activated carbon and its methylene blue adsorption capacity. Their life cycle assessment (LCA) findings offer valuable insights applicable to the current study. Using OpenLCA software and the TRACI method, they found that $K_2C_2O_4$ and KOH contribute significantly to global warming due to the higher quantities needed for carbon production, whereas $ZnCl_2$ and H_3PO_4 had lower environmental impacts. Specifically, H_3PO_4, demonstrated minimal environmental contributions in categories such as acidity, carcinogenicity, environmental toxicity, fossil fuel depletion, eutrophication, non-carcinogenicity, ozone depletion, respiratory effects, and smog formation.

These results corroborate the selection of H_3PO_4 as an activating agent in this study, highlighting its lower environmental footprint compared to other chemical activators. Thus, the activated carbon produced from murici seeds aligns with eco-friendly practices by minimizing negative environmental impacts during production. Furthermore, the potential for reusing spent adsorbents in multiple cycles or implementing inertization techniques could further reduce the environmental burden associated with their disposal. These findings support the relative sustainability of the activation process used in this work and highlight the importance of considering the full life cycle in future research.

While the use of H_3PO_4 presents environmental advantages, future studies could explore alternative activation methods that further minimize environmental impact. For instance, physical activation techniques, such as steam or CO_2 activation, eliminate the need for chemical reagents, reducing potential risks related to chemical handling and waste disposal. Additionally, bio-based activating agents derived from renewable resources, such as citric, tartaric, or fumaric acid, may offer greener alternatives. These natural acids not only reduce chemical waste but also lower the process's carbon footprint, aligning with sustainable development goals and reinforcing the environmental and economic viability of murici seed-derived activated carbon.

3.5. Management of used adsorbent

In this study, the used adsorbents after the adsorption of amoxicillin, phenol, and diethyl phthalate were discarded, as the base material (murici seeds) is low-cost, obtained as a donation from fruit processing companies, and the associated processing costs (water, energy, labor, and reagents) have been accounted for in other sections of this article. However, to enhance the sustainability of the process, future research should explore potential management strategies for spent adsorbents to minimize their environmental impact.

A viable option is the thermal regeneration of activated carbon, allowing for its reuse in multiple adsorption cycles and reducing the need for new material production. Nevertheless, this method presents limitations, such as the gradual decrease in adsorption capacity and the potential release of contaminants during the heating process. Alternatively, the saturated adsorbent could be repurposed as an alternative fuel, leveraging its energy content through controlled incineration. This approach, however, demands careful handling to prevent the emission of volatile pollutants. If disposal is unavoidable, inertization or deposition in specialized landfills is recommended to ensure that retained contaminants are securely contained and do not leach into the environment [15]. These strategies warrant further investigation to optimize the lifecycle of the adsorbents and promote a more sustainable approach.

To address the health and safety risks linked to H_3PO_4 usage during chemical activation, several mitigation strategies were considered. Implementing closed-system processes can significantly reduce operator exposure and prevent accidental acid releases into the environment. Moreover, post-activation neutralization—such as thoroughly washing the activated carbon with alkaline solutions—ensures the removal of residual acid, thereby minimizing environmental contamination risks. Additionally, the recycling of phosphoric acid solutions after activation can further reduce chemical waste and environmental impact. Exploring the use of less concentrated H_3PO_4 solutions could also mitigate health risks while maintaining activation efficiency. From an operational safety perspective, strict adherence to handling protocols, the use of appropriate personal protective equipment (PPE), and compliance with chemical safety regulations are critical for safeguarding personnel and maintaining safe working conditions. While phosphoric acid is generally less hazardous than other common activating agents, these precautionary measures are essential to ensuring both the environmental and occupational safety of the process.

4. Conclusion

Murici seed-based activated carbon, derived from agro-industrial residues and produced through an eco-friendly activation method using H_3PO_4, demonstrates significant potential for the removal of amoxicillin, phenol, and diethyl phthalate from aqueous media. This activated carbon exhibits a mesoporous structure with a substantial surface area of 556.97 $m^2.g^{-1}$ and a total pore volume that enhances its effectiveness as an adsorbent. The presence of acidic functional groups on its surface, along with a measured point of zero charge (pH_{PZC}) of 6.3, indicates its capacity to effectively interact with various contaminants based on their pKa values.

In adsorption experiments, murici activated carbon showed high adsorption capacities, achieving q_{max} values of 74.9 $mg.g^{-1}$ for phenol, 43.5 $mg.g^{-1}$ for diethyl phthalate, and 28.3 $mg.g^{-1}$ for amoxicillin. Notably, the kinetic analysis revealed that significant adsorption occurred within the first 60 minutes for all three contaminants, underscoring the rapid action of this material. The pseudo-second-order model provided the best fit for the adsorption data, suggesting that chemisorption is likely the predominant mechanism involved, facilitated by the acidic functional groups that enhance interactions between the adsorbent and pollutants.

Overall, these findings position murici activated carbon as a versatile and effective adsorbent for organic pollutant removal from aquatic systems. Its sustainable nature, remarkable adsorption properties, and quick adsorption kinetics highlight its potential applications in wastewater treatment, making it a valuable option for environmental protection and resource recovery efforts.

For future studies, the exploration of other agricultural waste sources as precursors for activated carbon production could expand the range of sustainable adsorbents available. Additionally, optimizing the activation process to further enhance adsorption performance or integrating murici-based activated carbon into composite adsorbents with synergistic properties could provide new avenues for improving pollutant removal efficiency. Evaluating its performance in real wastewater matrices and assessing potential regeneration and reuse strategies would also contribute to its practical application in large-scale water treatment systems.

5. Recommendations for future studies

To further advance the sustainable use of murici-based activated carbon, it is crucial to conduct a life cycle analysis (LCA) to assess the environmental advantages and disadvantages of its production process. This approach would provide a detailed view of the environmental impacts, from seed collection to the final disposal of used adsorbents. The LCA could be key to comparing murici-based activated carbon with other available alternatives, helping solidify its position as an eco-friendlier option for environmental remediation. Future studies could apply life cycle assessment tools, such as OpenLCA, to specifically evaluate the environmental footprint of murici seed-derived activated carbon, ensuring comprehensive sustainability metrics.

Additionally, it is recommended to investigate regeneration techniques for activated carbon, such as thermal or chemical regeneration, to evaluate their technical and economic feasibility. Regeneration could not only increase process efficiency by enabling the reuse of the adsorbent material but also help reduce operational costs in large-scale applications. Similarly, it would be valuable to explore more sustainable disposal methods for exhausted activated carbon, such as inertization or using the saturated material as an alternative fuel, provided that pollutant emissions are minimized.

Regarding process improvement, future research could focus on optimizing activation conditions, particularly by reducing the consumption of reagents and energy. For instance, investigating alternative activation methods, such as activation with CO_2 or steam, could make the process more sustainable and less dependent on chemicals like phosphoric acid.

The zeta potential analysis is a useful complementary technique to deepen the understanding of the interactions between pollutants and activated carbon. This technique would provide crucial information about the electrostatic stability of the particles and their tendency to form aggregates, offering a more detailed view of how specific functional groups on the surface of the carbon interact with the molecular structures of amoxicillin (AMX), phenol (PHE), and diethyl phthalate (DEP). Therefore, we suggest that a zeta potential analysis could be a valuable future approach to optimize adsorption conditions, improve process efficiency, and expand knowledge of surface interactions in aquatic systems.

To more comprehensively assess the viability of murici-based activated carbon in industrial applications, it would be valuable to conduct pilot or industrial-scale wastewater treatment system tests. These tests would not only evaluate its performance under more realistic conditions but also provide fundamental data on its effectiveness and potential limitations in a broader operational setting.

Since pH and temperature variations can significantly impact adsorption performance by altering the adsorbent's surface charge and the solubility of contaminants, we recommend that future studies include a more comprehensive analysis that combines different pH and temperature conditions. This approach would better simulate a wider range of real-world water treatment scenarios, offering deeper insights into how these factors influence adsorption efficiency and the feasibility of the process in practical applications.

Finally, it is suggested to perform a sensitivity analysis on carbonization temperature in future studies. This analysis could involve testing different temperatures and their impact on the physical and chemical properties of the activated carbon, as well as its adsorption capacity. This would allow for optimizing production conditions, further improving its performance as an adsorbent in water contamination remediation.

CRediT authorship contribution statement

Pereira Fernando: Resources, Methodology. **Pereira Julião:** Methodology. **Ferreira Tatianne:** Supervision, Resources, Funding acquisition, Conceptualization. **Alvez Tovar Beatriz Carolina:** Writing – review & editing, Visualization, Validation. **Alvares Taynara:** Writing – original draft, Methodology, Investigation, Data curation.

Declaration of Competing Interest

The authors declare that they have no known competing financial interests or personal relationships that could have appeared to influence the work reported in this paper

Acknowledgments

Our sincere appreciation goes to all participating investigators, the support provided by "CAPES" (Coordenação de Aperfeiçoamento de Pessoal de Nível Superior) and "PPGCTA" (Programa de Pós-Graduação em Ciência e Tecnologia de Alimentos) at the "UFG" (Universidade Federal de Goiás) for their infrastructure, the company "Frutos do Brasil" for donating the waste fruits, and the significant contributions from "GEERA" (Grupo de Estudos em Energias Renováveis e Ambiente) at "IFG" (Instituto Federal de Goiás) for their logistical support throughout this project.

Data Availability

Data will be made available on request.

References

[1] Santos VS, Vidal C, Bisinoti MC, Moreira AB, Montagner CC. Integrated occurrence of contaminants of emerging concern, including microplastics, in urban and agricultural watersheds in the State of São Paulo, Brazil. Sci Total Environ 2024; 932:173025. https://doi.org/10.1016/j.scitotenv.2024.173025.

[2] Rodríguez-Jiménez E, Cruz-Pérez N, García-Gil A, Roșca A, Díaz-Cruz MS, Santamarta JC. Contaminants of emerging concern in the duero river basin: presence and comparison between a nature reserve and an agricultural area. Groundw Sustain Dev 2024;26:101200. https://doi.org/10.1016/j.gsd.2024.101200.

[3] Sandoval MA, Calzadilla W, Vidal J, Brillas E, Salazar-González R. Contaminants of emerging concern: occurrence, analytical techniques, and removal with electrochemical advanced oxidation processes with special emphasis in Latin America. Environ Pollut 2024;345:123397. https://doi.org/10.1016/j.envpol.2024.123397.

[4] Puri M, Gandhi K, Kumar MS. Emerging environmental contaminants: a global perspective on policies and regulations. J Environ Manag 2023;332:117344. https://doi.org/10.1016/j.jenvman.2023.117344.

[5] Feng W, Deng Y, Yang F, Miao Q, Ngien SK. Systematic review of contaminants of emerging concern (CECs): distribution, risks, and implications for water quality and health. Water 2023;15:3922. https://doi.org/10.3390/w15223922.

[6] Ahmed SF, Mofijur M, Nuzhat S, Chowdhury AT, Rafa N, Uddin MdA, Inayat A, Mahlia TMI, Ong HC, Chia WY, et al. Recent Developments in physical, biological, chemical, and hybrid treatment techniques for removing emerging contaminants from wastewater. J Hazard Mater 2021;416:125912. https://doi.org/10.1016/j.jhazmat.2021.125912.

[7] Shirakami Y, Watabe T, Obata H, Kaneda K, Ooe K, Liu Y, Teramoto T, Toyoshima A, Shinohara A, Shimosegawa E, et al. Synthesis of [211at]4-astato-l-phenylalanine by dihydroxyboryl-astatine substitution reaction in aqueous solution. Sci Rep 2021;11:12982. https://doi.org/10.1038/s41598-021-92476-6.

[8] Osman AI, Hosny M, Eltaweil AS, Omar S, Elgarahy AM, Farghali M, Yap P-S, Wu Y-S, Nagandran S, Batumalaie K, et al. Microplastic sources, formation, toxicity and remediation: a review. Environ Chem Lett 2023;21:2129–69. https://doi.org/10.1007/s10311-023-01593-3.

[9] Landrigan PJ, Raps H, Cropper M, Bald C, Brunner M, Canonizado EM, Charles D, Chiles TC, Donohue MJ, Enck J, et al. The minderoo-monaco commission on plastics and human health. Ann Glob Health 2023;89:23. https://doi.org/10.5334/aogh.4056.

[10] Liu H, Hu Z, Liu H, Xie H, Lu S, Wang Q, Zhang J. Adsorption of amoxicillin by mn-impregnated activated carbons: performance and mechanisms. RSC Adv 2016;6: 11454–60. https://doi.org/10.1039/C5RA23256B.

[11] Kennedy LJ, Vijaya JJ, Kayalvizhi K, Sekaran G. Adsorption of phenol from aqueous solutions using mesoporous carbon prepared by two-stage process. Chem Eng J 2007;132:279–87. https://doi.org/10.1016/j.cej.2007.01.009.

[12] Medellin-Castillo NA, Ocampo-Pérez R, Leyva-Ramos R, Sanchez-Polo M, Rivera-Utrilla J, Méndez-Díaz JD. Removal of diethyl phthalate from water solution by adsorption, photo-oxidation, ozonation and advanced oxidation process (UV/H2O2, O3/H2O2 and O3/activated carbon). Sci Total Environ 2013;442:26–35. https://doi.org/10.1016/j.scitotenv.2012.10.062.

[13] Naddeo V, Secondes MFN, Borea L, Hasan SW, Ballesteros F, Belgiorno V. Removal of contaminants of emerging concern from real wastewater by an innovative hybrid membrane process – ultrasound, adsorption, and membrane ultrafiltration (USAMe®). Ultrason Sonochem 2020;68:105237. https://doi.org/10.1016/j.ultsonch.2020.105237.

[14] De Almeida MC, De Oliveira TF, De Sá FP. The elimination of cancerous pollutants by an advanced oxidation processes and adsorption in monosolute solutions mixtures in water. Desalin Water Treat 2020;191:292–9. https://doi.org/10.5004/dwt.2020.25710.

[15] Sanchez-Silva JM, Collins-Martínez VH, Padilla-Ortega E, Aguilar-Aguilar A, Labrada-Delgado GJ, Gonzalez-Ortega O, Palestino-Escobedo G, Ocampo-Pérez R. Characterization and transformation of nanche stone (byrsonima crassifolia) in an activated hydrochar with high adsorption capacity towards metformin in aqueous solution. Chem Eng Res Des 2022;183:580–94. https://doi.org/10.1016/j.cherd.2022.05.054.

[16] Laksaci H, Belhamdi B, Khelifi O, Khelifi A, Trari M. Elimination of amoxicillin by adsorption on coffee waste based activated carbon. J Mol Struct 2023;1274: 134500. https://doi.org/10.1016/j.molstruc.2022.134500.

[17] Mohamad Yusop MF, Abdullah AZ, Ahmad MA. Amoxicillin adsorption from aqueous solution by cu(ii) modified lemon peel based activated carbon: mass transfer simulation, surface area prediction and f-test on isotherm and kinetic models. Powder Technol 2024;438:119589. https://doi.org/10.1016/j.powtec.2024.119589.

[18] Choopani L, Salehi MM, Mashhadimoslem H, Khosrowshahi MS, Rezakazemi M, AlHammadi AA, Elkamel A, Maleki A. Removal of organic contamination from wastewater using granular activated carbon modified—polyethylene glycol: characterization, kinetics and isotherm study. PLOS ONE 2024;19:e0304684. https://doi.org/10.1371/journal.pone.0304684.

[19] Dos Santos HVR, Scalize PS, Teran FJC, Cuba RMF. Fluoride removal from aqueous medium using biochar produced from coffee ground. Resources 2023;12:84. https://doi.org/10.3390/resources12070084.

[20] Khan S, Naushad Mu, Govarthanan M, Iqbal J, Alfadul SM. Emerging contaminants of high concern for the environment: current trends and future research. Environ Res 2022;207:112609. https://doi.org/10.1016/j.envres.2021.112609.

[21] Morin-Crini N, Lichtfouse E, Fourmentin M, Ribeiro ARL, Noutsopoulos C, Mapelli F, Fenyvesi É , Vieira MGA, Picos-Corrales LA, Moreno-Piraján JC, et al. Removal of emerging contaminants from wastewater using advanced treatments. a review. Environ Chem Lett 2022;20:1333–75. https://doi.org/10.1007/s10311-021-01379-5.

[22] Osman AI, El-Monaem EMA, Elgarahy AM, Aniagor CO, Hosny M, Farghali M, Rashad E, Ejimofor MI, López-Maldonado EA, Ihara I, et al. Methods to prepare biosorbents and magnetic sorbents for water treatment: a review. Environ Chem Lett 2023;21:2337–98. https://doi.org/10.1007/s10311-023-01603-4.

[23] Espinosa Rodríguez MÁ, Delgado Delgado R, Hidalgo Millán A, Olvera Izaguirre L, Bernal Jácome LA. Adsorción de Cd(II) y Pb(II) Presentes En Solución Acuosa Con Hueso de Nanche (Byrsonima crassifolia). Rev Colomb QuíM 2020;49:30–6. https://doi.org/10.15446/rev.colomb.quim.v49n2.80633.

[24] Ashokkumar V, Flora G, Venkatkarthick R, SenthilKannan K, Kuppam C, Mary Stephy G, Kamyab H, Chen W-H, Thomas J, Ngamcharussrivichai C. Advanced technologies on the sustainable approaches for conversion of organic waste to valuable bioproducts: emerging circular bioeconomy perspective. Fuel 2022;324: 124313. https://doi.org/10.1016/j.fuel.2022.124313.

[25] Hajam YA, Kumar R, Kumar A. Environmental waste management strategies and vermi transformation for sustainable development. Environ Chall 2023;13:100747. https://doi.org/10.1016/j.envc.2023.100747.

[26] Mishra S, Yadav SS, Rawat S, Singh J, Koduru JR. Corn husk derived magnetized activated carbon for the removal of phenol and para-nitrophenol from aqueous solution: interaction mechanism, insights on adsorbent characteristics, and isothermal, kinetic and thermodynamic properties. J Environ Manag 2019;246: 362–73. https://doi.org/10.1016/j.jenvman.2019.06.013.

[27] Melo B, Alvez B, Otero D, Da Silva F, Scalize P, De Oliveira T. By-Products of baru and monguba: a review of their potential. Food Humanit 2024;4:100477. https://doi.org/10.1016/j.foohum.2024.100477.

[28] Ramutshatsha-Makhwedzha D, Mavhungu A, Moropeng ML, Mbaya R. Activated carbon derived from waste orange and lemon peels for the adsorption of methyl orange and methylene blue dyes from wastewater. Heliyon 2022;8:e09930. https://doi.org/10.1016/j.heliyon.2022.e09930.

[29] Guo S, Peng J, Li W, Yang K, Zhang L, Zhang S, Xia H. Effects of CO_2 activation on porous structures of coconut shell-based activated carbons. Appl Surf Sci 2009;255: 8443–9. https://doi.org/10.1016/j.apsusc.2009.05.150.

[30] Belaissa Y, Saib F, Trari M. Removal of amoxicillin in aqueous solutions by a chemical activated carbons derived from jujube nuts: adsorption behaviors, kinetic and thermodynamic studies. React Kinet Mech Catal 2022;135:1011–30. https://doi.org/10.1007/s11144-022-02159-0.

[31] Da Silva MCF, Lütke SF, Nascimento VX, Lima ÉderC, Silva LFO, Oliveira MLS, Dotto GL. Activated carbon prepared from brazil nut shells towards phenol removal from aqueous solutions. Environ Sci Pollut Res 2023;30:82795–806. https://doi.org/10.1007/s11356-023-28268-4.

[32] Sağlam S, Türk FN, Arslanoğlu H. Tetracycline (TC) removal from wastewater with activated carbon (ac) obtained from waste grape marc: activated carbon characterization and adsorption mechanism. Environ Sci Pollut Res 2024;31: 33904–23. https://doi.org/10.1007/s11356-024-33493-6.

[33] Strong OKL, France HE, Scotland K, Wright K, Vreugdenhil AJ. Selenite adsorption and reduction via iron(ii) impregnated activated carbon produced from the phosphoric acid activation of construction waste wood. Arch Environ Contam Toxicol 2023;85:485–97. https://doi.org/10.1007/s00244-023-01032-y.

[34] Dehmani Y, Lamhasni T, Mohsine A, Tahri Y, Lee H, Lgaz H, Alrashdi AA, Abouarnadasse S. Adsorption removal of phenol by oak wood charcoal activated carbon. Biomass– Convers Biorefinery 2024;14:8015–27. https://doi.org/10.1007/s13399-022-03036-5.

[35] Hu W, Zhang X, Chen M, Rahman ST, Li X, Wang G. Enhancing Cr (VI) adsorption of chestnut shell biochar through H_3PO_4 activation and nickel doping. Molecules 2024;29:2220. https://doi.org/10.3390/molecules29102220.

[36] Robles-Melchor L, Cornejo-Mazón M, Hernández-Martínez DM, Gutiérrez-López GF, García-Pinilla S, López-Villegas EO, Téllez-Medina DI. Removal of methylene blue from aqueous solutions by using nance (byrsonima crassifolia) seeds and peels as natural biosorbents. J Chem 2021;2021:1–13. https://doi.org/10.1155/2021/5556940.

[37] El-Bery HM, Saleh M, El-Gendy RA, Saleh MR, Thabet SM. High adsorption capacity of phenol and methylene blue using activated carbon derived from lignocellulosic agriculture wastes. Sci Rep 2022;12:5499. https://doi.org/10.1038/s41598-022-09475-4.

[38] Espinosa Rodríguez MÁ, Bernal-Jácome LA, Gallegos García M, Delgado-Delgado R, Olvera-Izaguirre L. Adsorption of Lead (Ii) from aqueous solution using adsorbents obtained from nanche stone (Byrsonima crassifolia). J Mex Chem Soc 2020;64. https://doi.org/10.29356/jmcs.v64i4.1201.

[39] Martins TA, De Sá FP, Pereira J, De Oliveira TF. Use of murici (byrsonima crassifolia) and jabuticaba (plinia cauliflora) residues in the preparation of porous materials: effect of ph on the adsorption efficiency of the contaminants phenol, diethylphthalate and amoxicillin. Desalin Water Treat 2024;317:100110. https://doi.org/10.1016/j.dwt.2024.100110.

[40] San-Martín-Hernández C, Martínez-Téllez MÁ, Valenzuela-Amavizca ON, Aispuro-Hernández E, Sánchez-Sánchez M, Hernández-Camarillo E, López-Martínez LX, Quintana-Obregón EA. *Byrsonima crassifolia* L. Kunth a bio-resource with potential: overview and opportunities. Folia Hortic 2023;35:61–75. https://doi.org/10.2478/fhort-2023-0005.

[41] Almeida CORP, Martinez RM, Figueiredo MS, Teodoro AJ. Botanical, Nutritional, Phytochemical Characteristics, and Potential Health Benefits of Murici (*Byrsonima crassifolia*) and Taperebá (*Spondias mombin*): Insights from Animal and Cell Culture Models. Nutr Rev 2024;82:407–24. https://doi.org/10.1093/nutrit/nuad065.

[42] Miki KSL, Dresch AP, Cavali M, Da Silva AP, Marafon F, Fogolari O, Mibielli GM, Bagatini MD, Bender JP. Influence of drying methods in the ultrasound-assisted

extraction of bioactive compounds from byrsonima crassifolia to evaluate their potential antitumor activity. Food Humanit 2024;2:100242. https://doi.org/10.1016/j.foohum.2024.100242.
[43] Sanchez-Silva JM, Ocampo-Pérez R, Padilla-Ortega E, Sangaré D, Escobedo-Bretado MA, Domínguez-Arvizu JL, Hernández-Majalca BC, Salinas-Gutiérrez JM, López-Ortiz A, Collins-Martínez V. Pyrolysis kinetics of byrsonima crassifolia stone as agro-industrial waste through isoconversional models. Molecules 2023;28:544. https://doi.org/10.3390/molecules28020544.
[44] National Center for Biotechnology Information. Diethyl Phthalate, PubChem Compound Summary for CID 6781 Available online: ⟨https://pubchem.ncbi.nlm.nih.gov/compound/Diethyl-Phthalate⟩ (accessed on 15 August 2024).
[45] National Center for Biotechnology Information. Amoxicilin, PubChem Compound Summary for CID 33613 Available online: ⟨https://pubchem.ncbi.nlm.nih.gov/compound/Amoxicillin⟩ (accessed on 15 August 2024).
[46] National Center for Biotechnology Information. Phenol, PubChem Compound Summary for CID 996 Available online: ⟨https://pubchem.ncbi.nlm.nih.gov/compound/Phenol⟩ (accessed on 15 August 2024).
[47] ChemSketch (Freeware) version 2023.2.4: ACD/Labs; Advanced Chemistry Development, Inc: Toronto, Canada, 2023. Available online: ⟨http://www.acdlabs.com⟩.
[48] Cagnon B, Chatelain S, De Oliveira TF, Versaveau F, Delpeux S, Chedeville O. Adsorption of phthalates on activated carbons in monosolute solution and in mix within complex matrices. Water Air Soil Pollut 2017;228:144. https://doi.org/10.1007/s11270-017-3315-7.
[49] Oginni O, Singh K, Oporto G, Dawson-Andoh B, McDonald L, Sabolsky E. Effect of One-Step and Two-Step H3PO4 activation on activated carbon characteristics. Bioresour Technol Rep 2019;8:100307. https://doi.org/10.1016/j.biteb.2019.100307.
[50] Neme I, Gonfa G, Masi C. Activated carbon from biomass precursors using phosphoric acid: a review. Heliyon 2022;8:e11940. https://doi.org/10.1016/j.heliyon.2022.e11940.
[51] Park J, Regalbuto JR. A simple, accurate determination of oxide PZC and the strong buffering effect of oxide surfaces at incipient wetness. J Colloid Interface Sci 1995;175:239–52. https://doi.org/10.1006/jcis.1995.1452.
[52] Horvat G, Pantić M, Knez Ž, Novak Z. A brief evaluation of pore structure determination for bioaerogels. Gels 2022;8:438. https://doi.org/10.3390/gels8070438.
[53] Kumar A, Gupta H. Activated carbon from sawdust for naphthalene removal from contaminated water. Environ Technol Innov 2020;20:101080. https://doi.org/10.1016/j.eti.2020.101080.
[54] González-García P. Activated carbon from lignocellulosics precursors: a review of the synthesis methods, characterization techniques and applications. Renew Sustain Energy Rev 2018;82:1393–414. https://doi.org/10.1016/j.rser.2017.04.117.
[55] Sánchez-Cantú M, Janeiro-Coronel VJ, Galicia-Aguilar JA, Santamaría-Juárez JD. Effect of the activation temperature over activated carbon production from castor cake and its evaluation as dye adsorbent. Int J Environ Sci Technol 2018;15:1521–30. https://doi.org/10.1007/s13762-017-1532-7.
[56] Sacco O, Vaiano V, Matarangolo M. ZnO supported on zeolite pellets as efficient catalytic system for the removal of caffeine by adsorption and photocatalysis. Sep Purif Technol 2018;193:303–10. https://doi.org/10.1016/j.seppur.2017.10.056.
[57] Zhuang X, Song Y, Zhan H, Bi XT, Yin X, Wu C. Pyrolytic conversion of biowaste-derived hydrochar: decomposition mechanism of specific components. Fuel 2020;266:117106. https://doi.org/10.1016/j.fuel.2020.117106.
[58] Duque-Brito E, Lobato-Peralta DR, Okolie JA, Arias DM, Sebastian PJ, Okoye PU. Fast-kinetics adsorption of a binary solution containing cationic and ionic pollutants using high-surface area activated carbon derived from macadamia nutshell. Energy Ecol Environ 2024;9:84–99. https://doi.org/10.1007/s40974-023-00304-6.
[59] Bakatula EN, Richard D, Neculita CM, Zagury GJ. Determination of point of zero charge of natural organic materials. Environ Sci Pollut Res 2018;25:7823–33. https://doi.org/10.1007/s11356-017-1115-7.
[60] Borel LDMS, Lira TS, Ribeiro JA, Ataíde CH, Barrozo MAS. Pyrolysis of brewer's spent grain: kinetic study and products identification. Ind Crops Prod 2018;121:388–95. https://doi.org/10.1016/j.indcrop.2018.05.051.
[61] Berges J, Moles S, Ormad MP, Mosteo R, Gómez J. Antibiotics removal from aquatic environments: adsorption of enrofloxacin, trimethoprim, sulfadiazine, and amoxicillin on vegetal powdered activated carbon. Environ Sci Pollut Res 2021;28:8442–52. https://doi.org/10.1007/s11356-020-10972-0.
[62] Cheng H, Zhang J, Chen Y, Zhang W, Ji R, Song Y, Li W, Bian Y, Jiang X, Xue J, et al. Hierarchical porous biochars with controlled pore structures derived from co-pyrolysis of potassium/calcium carbonate with cotton straw for efficient sorption of diethyl phthalate from aqueous solution. Bioresour Technol 2022;346:126604. https://doi.org/10.1016/j.biortech.2021.126604.
[63] Zhang L, Cheng H, Pan D, Wu Y, Ji R, Li W, Jiang X, Han J. One-pot pyrolysis of a typical invasive plant into nitrogen-doped biochars for efficient sorption of phthalate esters from aqueous solution. Chemosphere 2021;280:130712. https://doi.org/10.1016/j.chemosphere.2021.130712.
[64] Shi M, Wang X, Shao M, Lu L, Ullah H, Zheng H, Li F. Resource utilization of typical biomass wastes as biochars in removing plasticizer diethyl phthalate from water: characterization and adsorption mechanisms. Front Environ Sci Eng 2023;17:5. https://doi.org/10.1007/s11783-023-1605-4.
[65] Anastopoulos I, Pashalidis I, Orfanos AG, Manariotis ID, Tatarchuk T, Sellaoui L, Bonilla-Petriciolet A, Mittal A, Núñez-Delgado A. Removal of caffeine, nicotine and amoxicillin from (waste)waters by various adsorbents. a review. J Environ Manag 2020;261:110236. https://doi.org/10.1016/j.jenvman.2020.110236.
[66] Chandrasekaran A, Patra C, Narayanasamy S, Subbiah S. Adsorptive removal of ciprofloxacin and amoxicillin from single and binary aqueous systems using acid-activated carbon from Prosopis juliflora. Environ Res 2020;188:109825. https://doi.org/10.1016/j.envres.2020.109825.
[67] Shaida MohdA, Dutta RK, Sen AK. Removal of diethyl phthalate via adsorption on mineral rich waste coal modified with chitosan. J Mol Liq 2018;261:271–82. https://doi.org/10.1016/j.molliq.2018.04.031.
[68] Khraisheh M, Al-Ghouti MA, AlMomani FP. Putida as biosorbent for the remediation of cobalt and phenol from industrial waste wastewaters. Environ Technol Innov 2020;20:101148. https://doi.org/10.1016/j.eti.2020.101148.
[69] Leng L, Xiong Q, Yang L, Li H, Zhou Y, Zhang W, Jiang S, Li H, Huang H. An overview on engineering the surface area and porosity of biochar. Sci Total Environ 2021;763:144204. https://doi.org/10.1016/j.scitotenv.2020.144204.
[70] Liu H, Long L, Weng X, Zheng S, Xu Z. Efficient Removal of Tetrabromobisphenol A using microporous and mesoporous carbons: the role of pore structure. Microporous Mesoporous Mater 2020;298:110052. https://doi.org/10.1016/j.micromeso.2020.110052.
[71] Osman AI, Farrell C, Al-Muhtaseb AH, Harrison J, Rooney DW. The production and application of carbon nanomaterials from high alkali silicate herbaceous biomass. Sci Rep 2020;10:2563. https://doi.org/10.1038/s41598-020-59481-7.
[72] El Azzouzi L, El Aggadi S, Ennouhi M, Ennouari A, Kabbaj OK, Zrineh A. Removal of the amoxicillin antibiotic from aqueous matrices by means of an adsorption process using kaolinite clay. Sci Afr 2022;18:e01390. https://doi.org/10.1016/j.sciaf.2022.e01390.
[73] Xie B, Qin J, Wang S, Li X, Sun H, Chen W. Adsorption of phenol on commercial activated carbons: modelling and interpretation. Int J Environ Res Public Health 2020;17:789. https://doi.org/10.3390/ijerph17030789.
[74] Elsayed AE, Attia SK, Rashad AM, Mahmoud GA, Osman DI. Synthesis of dispersed magnetic Fe3O4 nanohydrogel based on gelatine by gamma irradiation for toxic heavy metals removal. J Inorg Organomet Polym Mater 2024. https://doi.org/10.1007/s10904-024-03387-8.
[75] Choudhry Q, Fan M, Sun K, Li B, Zhang S, Kousar S, Khan ZE, Hu X. Chemical activation of cotton fibers with varied regents induces distinct morphology of activated carbon and adsorption capacity of methylene blue. Int J Biol Macromol 2025;295:139657. https://doi.org/10.1016/j.ijbiomac.2025.139657.